

Host traits and environment interact to drive host-pathogen coexistence following pathogen invasion

Alexander Grimaudo¹, Joseph Hoyt¹, Steffany Yamada¹, Carl Herzog², Alyssa Bennett³, and Kate Langwig¹

¹Virginia Tech

²New York State Department of Environmental Conservation

³Vermont Fish and Wildlife Department

July 16, 2021

Abstract

Emerging infectious diseases have resulted in severe population declines across diverse taxa. In some instances, despite attributes associated with high extinction risk, disease emergence and host declines are followed by host stabilization for reasons that are frequently unclear. While host, pathogen, and the environment are recognized as important factors that interact to determine host-pathogen coexistence, they are often considered independently. Here, we use a translocation experiment to disentangle the role of host traits and environmental conditions in driving the persistence of remnant populations a decade after they declined 70-99% and subsequently stabilized with disease. While survival was significantly higher than during the initial epidemic within all sites, protection from severe disease only existed within a narrow environmental space, suggesting host traits conducive to surviving disease are highly environmentally dependent. Ultimately, population persistence following pathogen invasion is the product of host-pathogen interactions that vary across a patchwork of environments.

Title: Host traits and environment interact to drive host-pathogen coexistence following pathogen invasion

Running title: Mechanisms of host-pathogen coexistence

Manuscript format: Nature

Article type: Letter

Author line: Alexander T. Grimaudo¹, Joseph R. Hoyt¹, Steffany A. Yamada¹, Carl J. Herzog², Alyssa B. Bennett³, and Kate E. Langwig¹

Affiliation: ¹Department of Biological Sciences, Virginia Tech, Blacksburg, Virginia, 24060. ²New York State Department of Environmental Conservation, Albany, New York, 12233. ³Vermont Fish and Wildlife Department, Montpelier, Vermont, 05602

Corresponding author: at.grimaudo@gmail.com, Steger Hall Room 363-3, 1015 Life Science Circle, Blacksburg, Virginia 24061

Statement of authorship: Conceptualization, ATG, JRH, and KEL; Methodology, ATG, JRH, and KEL; Formal Analysis, ATG and KEL; Investigation, ATG, JRH, SAY, CJH, ABB, and KEL; Data Curation, ATG, JRH, and KEL; Writing – Original Draft, ATG; Writing – Review & Editing, ATG, JRH, SAY, CJH, ABB, and KEL; Visualization, ATG; Supervision, JRH and KEL; and Project Administration, JRH and KEL.

Data accessibility statement: Should our manuscript be accepted, the data supporting the results will be archived in Dryad and the data DOI will be included at the end of the article

Keywords: temperature-mediated effects; host-pathogen coexistence; geographic mosaics; eco-evolutionary dynamics; emerging infectious disease; host resistance; host tolerance

Words in abstract: 188

Words in main text: 4,683

References: 123

Figures: 5

ABSTRACT

Emerging infectious diseases have resulted in severe population declines across diverse taxa. In some instances, despite attributes associated with high extinction risk, disease emergence and host declines are followed by host stabilization for reasons that are frequently unclear. While host, pathogen, and the environment are recognized as important factors that interact to determine host-pathogen coexistence, they are often considered independently. Here, we use a translocation experiment to disentangle the role of host traits and environmental conditions in driving the persistence of remnant populations a decade after they declined 70-99% and subsequently stabilized with disease. While survival was significantly higher than during the initial epidemic within all sites, protection from severe disease only existed within a narrow environmental space, suggesting host traits conducive to surviving disease are highly environmentally dependent. Ultimately, population persistence following pathogen invasion is the product of host-pathogen interactions that vary across a patchwork of environments.

INTRODUCTION

Emerging infectious diseases of wildlife have resulted in severe mortality events and regional to complete extinctions of host populations¹⁻⁶. In some instances, the presence of pathogen reservoirs, frequency-dependent transmission, and small pre-epidemic host population sizes suggest that host species will be driven to extinction⁷. Additionally, high initial host population declines leave remnant populations more vulnerable to stochastic and Allee effects that increase the likelihood of host extinction⁷⁻⁹. However, following the initial epidemic and population declines, some host populations stabilize and persist for unknown reasons^{3,10,11}. For example, population persistence has been observed in several important disease systems including amphibians impacted by chytridiomycosis¹⁰⁻¹⁴, Tasmanian devils impacted by facial tumor disease¹⁵⁻¹⁸, birds impacted by avian malaria¹⁹, and bats impacted by white-nose syndrome^{3,20}. While initial evidence suggested that these host populations would be extirpated by infectious disease, some populations have stabilized despite infection prevalence remaining high while others continue to decline or have gone extinct^{3,5,26,10,11,16,21-25}.

Potential drivers of host-pathogen coexistence include the evolution of host resistance, tolerance, and/or general vigor²⁷⁻³⁵, environmental refugia from infection or severe disease³⁶⁻⁴¹, host demographic compensation^{13,42-45}, density-dependent transmission⁴⁶⁻⁴⁹, and attenuation of pathogen virulence⁵⁰⁻⁵⁵. However, studies investigating host coexistence with virulent pathogens frequently focus on a single aspect of the host-pathogen-environment interaction, which may provide incomplete information on how host populations actually persist with disease. Given that many mechanisms of host population persistence include interactions between hosts and the environment, which may change as pathogen invasion progresses, understanding these interactions is essential for identifying the conditions necessary for host-pathogen coexistence following the invasion of a virulent pathogen.

White-nose syndrome (WNS) is an infectious disease of bats caused by the fungal pathogen *Pseudogymnoascus destructans*⁵⁶⁻⁵⁸. In North America, the disease was first detected in New York state in 2006⁵⁹ and has since resulted in large mortality events and regional extinctions of once common bat species^{3,21,24}. Bats become infected with *P. destructans* upon entering hibernacula in the fall⁶⁰, and both indirect and direct transmission result in widespread infection early in the seasonal epidemic^{22,56,60,61}. An environmental

pathogen reservoir is established following the introduction of the pathogen to a hibernaculum^{22,62} and most populations decline greater than 90%, often resulting in complete local extirpations^{3,63}. However, bats that survive hibernation emerge onto the landscape in spring and clear infection^{60,64,65}.

The growth of *P. destructans* is sensitive to environmental temperature⁶⁶ and humidity⁶⁷, resulting in environmental trends in population declines such that populations and species roosting in warmer and wetter environments have more severe declines^{3,24,68–70}. However, several years following pathogen introduction, some colonies of little brown bats (*Myotis lucifugus*) in the northeast United States stabilized at 5-30% of their pre-epidemic population size following cumulative regional declines of 96%^{3,21,23,71,72} despite infection prevalence remaining high⁷². The isolate of *P. destructans* collected from bats following its introduction to North America reproduces asexually^{73,74}, and genetic evidence indicates the pathogen has changed little since the initial introduction^{73,75}, suggesting virulence attenuation is not likely the principal driver of host-pathogen coexistence in this system. Additionally, the abiotic pathogen reservoir within hibernacula sustains a high prevalence of infection regardless of colony size, suggesting density-dependent transmission is also not a driver of population persistence^{22,60,76,77}. Compared to colonies undergoing epidemic conditions on the invasion front, bats in persisting colonies display slower on-host pathogen growth rates, potentially a signature of host resistance⁷². However, persisting colonies also utilize colder hibernacula^{3,69}, so lower pathogen growth rates may be a product of temperature operating independently of host characteristics.

The relative role of host traits and environmental conditions in driving the persistence of little brown bat populations impacted by WNS is still unclear. Understanding the factors driving host persistence will provide empirical support for general theory on host coexistence with virulent pathogens and much needed information on this important and devastating wildlife disease. Ten years following the introduction of *P. destructans* and subsequent colony declines, we conducted a fully factorial translocation experiment to understand the mechanisms of population persistence. We leveraged the variable environmental conditions in hibernacula (Fig. 1, Supplemental Fig. 1, 2) and a previously conducted translocation experiment early in the epizootic to disentangle the relative roles of host traits and environmental conditions in driving disease severity and ultimately population persistence.

RESULTS

Summary

Bats were translocated between two hibernacula with persisting colonies as well as to one hibernaculum previously extirpated of bats by WNS (Fig. 1). Bats were caged within each site, where they remained for the duration of winter, allowing us to quantify disease severity from the same individuals at both the beginning and end of hibernation. In all three sites, survival observed during the translocation experiment was higher than that observed within the same sites during the initial epidemic. This suggests little brown bats in persisting colonies have unique host traits that promote surviving infection with *P. destructans*. However, disease severity and subsequently survival varied across the three hibernacula, suggesting environmental conditions interact with host traits to ultimately drive persistence.

Pathogen growth rate

At the time of collection in early hibernation, 88.89% (n=40) of individuals from Persisting 1 (Cold + Dry) had detectable *P. destructans* from swab samples, as did 97.78% (n=44) from Persisting 2 (Cold + Wet). All cages in each site had at least one infected bat at the beginning of the experiment. Additionally, at the time of collection, bats captured in Persisting 1 (Cold + Wet) had higher pathogen loads than bats that originated in Persisting 2 (Cold + Dry) (generalized linear model with gamma error distribution and log link function: $\beta = 1.371 \pm 0.428$ SE, $p = 0.002$; Supplemental Fig. 3).

Over the course of the experiment, the highest on-host pathogen growth rates were recorded in the previously extirpated site (Warm + Wet), which was at least 4° C warmer than either of the two persisting sites, on average. Pathogen growth rates in Persisting 2 (Cold + Wet) were slightly higher than in Persisting 1 (Cold + Dry), likely attributable to the 1° C warmer and more humid conditions in the former. We also detected an

interactive effect of origin site (the site from which bats were collected at the beginning of the experiment) and translocation site on the pathogen growth rate, such that within the previously extirpated site (Warm + Wet), bats originating in Persisting 2 (Cold + Wet) had lower pathogen growth rates than bats that originated in Persisting 1 (Cold + Dry) (Fig. 2; Supplemental Table 1). Correspondingly, we detected an interactive effect of average roosting temperature and origin site on pathogen growth rate (Fig. 2; Supplemental Table 2). Across all bats, the pathogen growth rate increased with average roosting temperature, consistent with the sensitivity of *P. destructans* to ambient thermal conditions^{24,66}. However, due to the effect of origin site, the estimated relationship between average roosting temperature and pathogen growth rate was positive for bats that originated in Persisting 1 (Cold + Dry) but did not increase for bats that originated in Persisting 2 (Cold + Wet) (Fig. 2). Interestingly, we observed a decrease in pathogen loads on five bats in Persisting 1 (Cold + Dry), four in Persisting 2 (Cold + Wet), and one in Extirpated (Warm + Wet).

Infection severity and host body condition

The degree of tissue invasion and weight loss varied across the three sites (Fig. 3). Corresponding to the temperature-dependent pathogen growth rate, the severity of infection at Extirpated (Warm + Wet) was significantly higher than that observed at the similarly wet site, Persisting 2 (Cold + Wet) (Fig. 3A; Supplemental Table 3). However, contrary to the temperature-dependent pathogen growth rate observed, bats at Persisting 1 (Cold + Dry) displayed significantly higher infection severity than that observed at Persisting 2 (Cold + Wet) and did not significantly differ from that observed in Extirpated (Warm + Wet). This pattern of tissue invasion was mirrored by the degree of weight loss observed across the sites, as bats in Persisting 2 (Cold + Wet) had lower weight loss compared to either of the other sites (fig. 3B; Supplemental Table 4). The particularly dry conditions within Persisting 1 (Cold + Dry) may have resulted in the deviation from the temperature-pathogen growth relationship, exacerbating infection severity and weight loss despite a relatively low level of pathogen growth.

Survival

The highest survival was observed in Persisting 2 (Cold + Wet) (29 survivors of 30, 96.67% surviving), mirroring the pattern of infection severity and host body condition (Fig. 4; Supplemental Table 5). The lowest observed survival occurred in Persisting 1 (Cold + Dry) (12 survivors of 30, 40% surviving) while Extirpated (Warm + Wet) displayed an intermediate level of survival (24 survivors of 30, 80% surviving). We found no effect of early hibernation body mass on survival (Supplemental Table 6). The higher degree of mortality at Extirpated (Warm + Wet) may have been related to the high pathogen growth rate within the site, while the high mortality at Persisting 1 (Cold + Dry) may be attributable to the particularly dry conditions, which appeared to exacerbate infection severity. Additionally, low humidity conditions increase evaporative water loss during infection with *P. destructans*⁷⁸, so the high degree of mortality within the cold and dry site may be attributable to the high infection severity driving higher rates of water loss^{78–84}. However, in all sites, the level of survival observed was higher than that observed during the initial epidemic within the same sites, suggesting traits adaptive to surviving WNS are promoting persistence in these populations (Fig. 4).

An additional line of evidence for adaptive traits promoting persistence in this system comes from a similar study in 2009 in which bats naïve to WNS were translocated to the same extirpated site used in this study. In the historical experiment, all experimental bats died within 114 days (compared to 110 days, the length of this experiment; Supplemental Fig. 4).⁸⁵ Effectively, this represents two replicates of extirpation within this site, in which all naïve bats succumbed to disease during the initial epidemic and subsequent re-introduction in 2009. However, in this translocation experiment, 24 of the 30 (80%) little brown bats we translocated from persisting colonies to the same extirpated site survived hibernation, suggesting these populations now have traits adaptive to surviving infection. Additionally, compared to the bats in the extirpated site during the historical translocation experiment, bats in our study had low disease severity scores as indicated by UV fluorescence (Supplemental Fig. 5).

Comparisons with free-flying bats

At the end of the experiment in late hibernation, we sampled free-flying bats found roosting near the cages within each persisting site. At Persisting 1 (Cold + Dry), we found that free-flying bats had significantly lower tissue invasion compared to the bats within cages (Fig. 5; Supplemental Table 7). Conversely, free-flying bats at Persisting 2 (Cold + Wet) displayed a similar degree of infection severity to caged bats within the same site. Free-flying bats had higher late hibernation body mass than caged bats in both persisting sites (Supplemental Fig. 6; Supplemental Table 8), and this difference was more pronounced in Persisting 1 (Cold + Dry).

DISCUSSION

Our data suggest that environmental conditions interact with host traits to jointly drive persistence of host populations. We found evidence for elevated on-host growth of *P. destructans* with increasing roosting temperature in bats that originated in Persisting 1 (Cold + Dry), but no relationship in bats that originated in Persisting 2 (Cold + Wet). Infection severity, host body condition, and survival also appeared to be influenced by site humidity, with higher disease severity and lower survival associated with over-winter exposure to the driest conditions in Persisting 1 (Cold + Dry). However, within the dry conditions, bats sampled from outside of cages in late hibernation displayed significantly lower infection severity compared to their caged counterparts, whereas no such difference was detected in Persisting 2 (Cold + Wet). This suggests that bats within Persisting 1 (Cold + Dry) may be utilizing a variety of microclimates and not remaining in these dry environments for the entire winter period, as the caged bats experienced. Importantly, the survival we observed during this experiment was significantly higher than survival during the initial epidemic within the same sites in all cases, as well as during a similar experiment in 2009. Furthermore, we observed declines in pathogen loads on 10 individuals, nine of which were in persisting sites. These data collectively suggest that persisting little brown bat colonies in the northeast United States have evolved traits beneficial to surviving WNS^{88,89}, but that these host traits interact with environmental conditions such that protection against severe disease and mortality depends to a strong degree on temperature and humidity.

We detected a positive relationship between average roosting temperature during hibernation and on-host pathogen growth rate. This is corroborated by data from the initial WNS epidemic, where the most severely impacted colonies were those hibernating in relatively warm hibernacula³. Infection severity and over-winter weight loss showed a similar trend when humidity was high, with lower values occurring at Persisting 2 (Cold + Wet) compared to Extirpated (Warm + Wet). However, despite the coldest ambient conditions, infection severity and host weight loss were high under the dry conditions within Persisting 1 (Cold + Dry) and were comparable to the extirpated site. Under unfavorable ambient conditions, fungal pathogens may forgo reproduction and instead commit resources to within-host growth and the formation of spores that can survive stressful conditions. For example, *Metarhizium anisopliae* is a fungal pathogen of tick eggs that invades the egg tissue and undergoes growth^{90,91}. Under humid, favorable conditions, the fungus will emerge from the egg to undergo asexual reproduction. However, under dry, unfavorable conditions, the fungus will instead remain within the egg host, continue to undergo growth, and produce environmentally resistant spores⁹¹. We suggest that, similarly, exposure to dry conditions of Persisting 1 (Cold + Dry) over winter were unfavorable to the survival of *P. destructans* in superficial infections, and that the pathogen augmented tissue invasion to satisfy moisture requirements, resulting in a high degree of infection severity. Additionally, evaporative water loss from hibernating bats is highest in dry conditions^{92,93} and is exacerbated by infection with *P. destructans*⁷⁸, resulting in dehydration and increased arousal frequency to re-hydrate⁷⁸⁻⁸⁴. Increased frequency of arousal from torpor drives the premature depletion of fat reserves during hibernation, resulting in weight loss and starvation^{58,94}. Therefore, the increased tissue invasion and evaporative water loss in Persisting 1 (Cold + Dry) may have operated synergistically to result in severe disease and ultimately the lowest observed survival.

Colonies of little brown bats in dry hibernacula may be persisting because of the availability of different microclimates. Microclimatic conditions are not uniform throughout an entire hibernation site, but vary with factors such as depth, air flow, and the height of the ceiling⁹⁵. Recent evidence suggests that bats may arouse and move to different roosting locations periodically during hibernation⁹⁶, possibly in response to

shifting costs associated with hibernation⁹⁷, which could expose them to a variety of microclimates⁹⁸. For example, some data suggest that bats may transition from roosting in relatively warm sections of hibernacula in early hibernation to the relatively cold sections by late winter⁹⁶. In our study, bats were unable to select varying microclimates over the course of hibernation. However, we observed hundreds of little brown bats roosting in the area surrounding the cages during late winter in Persisting 1 (Cold + Dry), whereas less than a dozen individuals appeared to use that specific location in early hibernation, suggesting that bats do not roost in the same location for the entirety of hibernation in this site. Given that disease severity is highly dependent on environmental conditions within hibernacula, this movement behavior may have been pre-adaptive to surviving WNS if bats utilize microclimates that mitigate disease severity for at least part of hibernation. For example, movement within hibernacula may reduce the growth of *P. destructans* in late hibernation if bats move to the relatively cold conditions that slow pathogen growth, potentially affording them enough time to emerge from hibernation in spring and clear infection. Within Persisting 1 (Cold + Dry), free-flying bats sampled at the end of hibernation had significantly lower infection severity than caged bats, which is the expected pattern if movement within hibernacula is indeed beneficial to mitigating disease severity. Furthermore, free-flying bats in both persisting sites had higher late hibernation body masses, and this was more pronounced in Persisting 1 (Cold + Dry). Behavioral responses that moderate the severity of disease have also been proposed for snake populations impacted by snake fungal disease⁹⁹, caused by the fungal pathogen *Ophidiomyces ophiodiicola*¹⁰⁰. Snakes infected with *O. ophiodiicola* exhibit changes to their behavior that include increased surface activity and more time spent in exposed environments compared to their disease-free conspecifics^{99,100}, potentially a sign of a behavioral fever response to infection¹⁰¹. However, we make the important distinction here that because movement within hibernacula was observed in bats prior to the WNS epidemic, this behavior may have been pre-adaptive to surviving the disease rather than a direct response to the disease itself. Future research should investigate how the availability and utilization of varying environmental conditions can influence the dynamics of WNS, and how this may scale up to a population-level response.

During the initial epidemic, the cold conditions within hibernacula utilized by colonies may have prevented total colony collapse, allowing standing genetic variation for favorable host traits to propagate^{3,24,68,70,102}. Previous research has also found genetic evidence from persisting little brown bat colonies indicative of a selective sweep following the invasion of *P. destructans*^{89,103}. However, our data suggest that populations that appear to have evolved adaptive host traits are only afforded protection within a narrow environmental space. These processes have the potential to result in local adaptation, in which the evolutionary response of populations to WNS and the resulting dominant phenotype is specific to the local environmental conditions of hibernacula¹⁰⁴. We detected an effect of origin site on pathogen growth rate within Extirpated (Warm + Wet), potentially a signature of local adaptation to differing conditions in source hibernacula. However, for local adaptation to occur, the strength of selection must be high enough to combat the homogenizing effects of gene flow^{105–108}, and current genetic evidence suggests a panmictic genetic landscape for bat populations^{109–113}, but see^{114,115}.

Environmental conditions within hibernacula are sensitive to conditions present aboveground⁹⁵, and global climate change has the potential to alter the host-pathogen interaction in this system^{116,117}. Disease severity is strongly linked to temperature and humidity conditions, as is the protection afforded by unique host traits, as this study suggests. Therefore, even slight changes to the environmental conditions within hibernacula may alter host survival within a given site, potentially resulting in more severe disease and higher mortality if conditions deviate from the environmental space within which bats coexist with the pathogen. Future research should explore the potential for climate change to impact the disease dynamics of WNS, as well as the potential for bat populations to respond to shifting conditions.

As *P. destructans* continues to spread throughout North America, bat population declines and regional extirpations will continue to occur. However, this study strongly suggests that prior to the invasion of *P. destructans*, host traits conducive to surviving WNS circulated in little brown bat populations, which now offer some colonies imperfect protection from the disease. These host traits do not operate independently to promote population persistence with WNS, but rather interact strongly with environmental conditions,

specifically temperature and humidity, to ultimately drive host-pathogen coexistence. Therefore, we should not expect to see all little brown bat populations across North America stabilize or rebound from declines, but rather the persistence of colonies with the correct combination of host traits and environmental conditions.

Host population response to the invasion of a virulent pathogen will not be predictable by a single aspect of the host, environment, or pathogen. Rather, host-pathogen interactions and coexistence will be strongly mediated by environmental conditions, the result of which may be as variable as the environment itself^{118,119}. Underlying variation in host and pathogen populations will set the stage for subsequent coevolutionary processes and the likelihood of coexistence^{102,120}, but this interaction and the resulting host population response may be influenced by environmental conditions that vary over space and time^{118,121}, as illustrated by this study. Therefore, to achieve predictability in how emerging infectious diseases will impact host populations, it is essential to disentangle host-environment-pathogen interactions across a geographic and temporal mosaic of host-pathogen coevolution.

MATERIALS AND METHODS

Translocation experiment

Two known hibernacula of persisting little brown bat (*Myotis lucifugus*) colonies in New York and one hibernaculum previously extirpated of bats by white-nose syndrome (WNS) in Vermont were used in this study (Fig. 1). Prior to the beginning of the hibernation season, we installed ten, five-sided reptile cages (dimensions: 12”W, 18”L, 20”H; ZillaRules, Wisconsin, USA) in known or historical roosting locations within each site (Supplemental Fig. 7). Each cage was mounted so that the open side was in contact with the hibernaculum surface, allowing bats to roost directly on the substrate. Cages were mounted high on site ceilings and were sealed to prevent predation of bats. Poultry waterers were placed in each cage to provide a water source.

At the beginning of December 2018, in early hibernation, we returned to the two sites of persisting *M. lucifugus* colonies in New York. We collected 45 male *M. lucifugus* from each site and fitted them with a unique forearm band. Each individual was randomly assigned to both a site and a cage within that site with 3 individual bats from the same origin site sharing each cage. These assignments were in a full factorial design, such that of the 45 bats collected from each site, 15 were assigned to be caged within the same site, 15 to be caged within the opposite persisting site, and 15 to be caged in the previously extirpated site. We placed each bat individually in a cloth bag and transported them to their assigned site in a cooler so that they would remain in torpor and limit energy expenditure. We replicated the transportation disturbance across all treatment groups. Bats remained in their assigned cages for the duration of hibernation. All individuals were caged with at least one infected individual. In mid-hibernation, each of the three sites were visited once to record survival status through visual inspection (Persisting 1: 50 days; Persisting 2: 64 days; Extirpated: 71 days following initial translocation); no cages were opened or bats handled, as to minimize disturbance. In March 2019, in late hibernation, 110 days following the initial translocation, we returned to each of the three sites to collect data and terminate the experiment. We released all surviving individuals at their site of origin.

Disease severity metrics

Upon returning to each of the three sites, we recorded the survival status of each individual. To calculate the on-host pathogen growth rate of *Pseudogymnoascus destructans*, we collected swab samples from each individual bat in both December 2018 and March 2019 using a standardized swabbing protocol described in⁶⁰. Swab samples were preserved in RNAlater until extraction. We used real-time polymerase chain reaction (qPCR) targeting the multicopy intergenic spacer region of the rRNA gene complex to test swab samples for the presence of *P. destructans* DNA¹²². We measured the quantity of *P. destructans* DNA in picograms from each swab sample based on the cycle threshold (C_t) value with a C_t cutoff of 40 cycles and a previously described standard quantification curve described in²⁴.

In both December 2018 and March 2019, we weighed each individual bat using an electronic scale. We

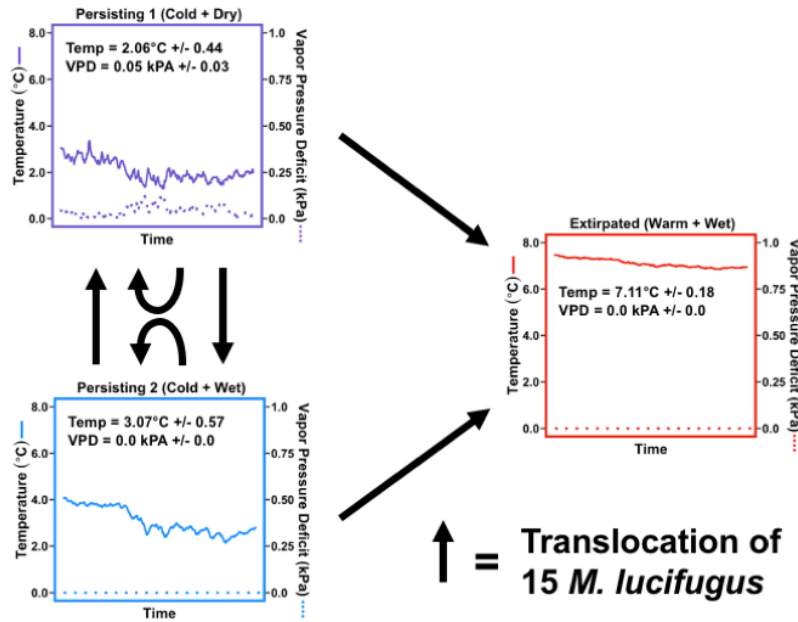
subtracted the late hibernation weight of each individual from their early hibernation weight to calculate the amount of weight lost over the course of hibernation in grams. Additionally, in March 2019, we collected data on the severity of tissue invasion by transilluminating both wings of each individual using a 9-watt 368nm fluorescent light (BRC-100, Way Too Cool LLC, from www.fluorescents.com). Infected tissue fluoresces orange when exposed to ultraviolet light and has been verified by histology⁸⁷. During transillumination, we photographed each wing using a Canon (Tokyo, Japan) EOS Rebel T6 (AF 15-55 mm lens, F-stop 22, ISO 1600, shutter speed 2.5 seconds, no filter). We used Adobe (San Jose, USA) Photoshop Elements Editor 15 to quantify the proportion of the plagiopatagium of each wing that displayed orange fluorescence indicative of infection with *P. destructans*. We first calculated the total number of pixels encompassed by the plagiopatagium, excluding bone area or area obstructed by fur. Then, we calculated the total number of orange pixels within the plagiopatagium. For each bat, pixel values from both wings were summed and proportions derived from these values. These image analyses were done by an individual blind to the origin of each bat and the hypotheses and predictions of the study.

Statistical analysis

We conducted all analyses using package “lme4”¹²³ in R v.3.6.0 (R Core Team 2019). We constructed separate models for each disease severity metric, each of which included an interactive term of site*origin site (“origin site” was the site from which bats were collected at the beginning of the experiment, whereas “site” was that within which bats were ultimately caged) as the predictor variable and a unique cage ID as a random effect. Pathogen growth rate was the only disease severity metric with a significant effect of origin site, so we report the effect for this metric but drop the origin site term in the other models. In all analyses, we only used data from alive bats except for analyses on tissue invasion. We did not use pathogen load data from dead bats because *Pseudogymnoascus destructans* is a poor competitor on bat carcasses and, therefore, swab data from dead bats does not accurately convey the pathogen load at the time of mortality.

To measure pathogen growth rate for each individual bat, we subtracted its early hibernation fungal load value from its late hibernation value to quantify the change in fungal loads. Bats that had no detectable fungus at the time of swabbing were assigned a value of $4.35e-03$ pg (equivalent to a C_t value of 40) for that swab sample²⁴, or a single *P. destructans* conidia. We then added a constant of 10 and log10-transformed the growth rate values. We used a linear regression to assess the differences in change in fungal loads on bats at each site. Incorporating cage ID as a random effect did not add explanatory power to this model and was dropped. In addition, to understand the relationship between roosting temperature and the change in fungal loads, we constructed a separate linear mixed model with the average roosting temperature (data collected by iButtons within each cage), origin site, and their interaction as fixed effects and cage ID as a random effect.

To test for differences in the severity of tissue invasion across the sites, we used a logistic regression with orange pixels indicating infection as successes and non-orange pixels as failures (generalized linear mixed model with binomial error distribution and logit link function), site as a fixed effect, and cage ID as a random effect. Additionally, to test for differences in tissue invasion between caged bats and free-flying bats opportunistically sampled at the end of hibernation in each of the persisting sites, we used a logistic regression with the same response variable (generalized linear mixed model with binomial error distribution and logit link function) and site, caging status (caged vs. free-flying), and their interaction as fixed effects. To explore the differences in weight loss across the three sites, we used a generalized linear mixed model (gamma error distribution, log link function) with weight loss as the response variable, translocation site as a fixed effect, and cage ID as a random effect. To test for differences in late hibernation body mass between caged and free-flying bats in each persisting site, we used a multiple linear regression with body mass as the response variable and an interaction term of site and caging status as the explanatory variable. We used a generalized linear mixed model (binomial error distribution, logit link function) to explore the relationship between early hibernation body mass and survival. Finally, we used a generalized linear mixed model (binomial error distribution, logit link function) to investigate how survival varied across the sites.



FIGURES

FIGURE 1: Schematic of the experimental design. Two sites in New York with known persisting colonies of little brown bats and one site that was previously extirpated of little brown bats were used in this study. The three sites are referred to as Persisting 1 (Cold + Dry), Persisting 2 (Cold + Wet), and Extirpated (Warm + Wet). Solid and dashed lines on plots correspond to temperature (Celsius) and vapor pressure deficit (kPa; higher values correspond to drier conditions), respectively, within each site over the course of this study. Mean \pm SD of temperature and vapor pressure deficit within each site is shown on each plot. Sites varied in their environmental conditions, with the persisting sites being colder than the extirpated site and Persisting 1 (Cold + Dry) being significantly drier than Persisting 2 (Cold + Wet). Persisting 2 (Cold + Wet) was similar in its humidity conditions to Extirpated (Warm + Wet). In early hibernation, 45 bats from each of the persisting sites ($n = 90$) were collected and randomly assigned a translocation site and cage (3 bats per cage). The translocation was fully factorial, with 15 bats from each site being caged within the same site, in the opposite persisting site, or the extirpated site. Bats remained caged within these sites until late hibernation, when survivors were returned to their site of origin.

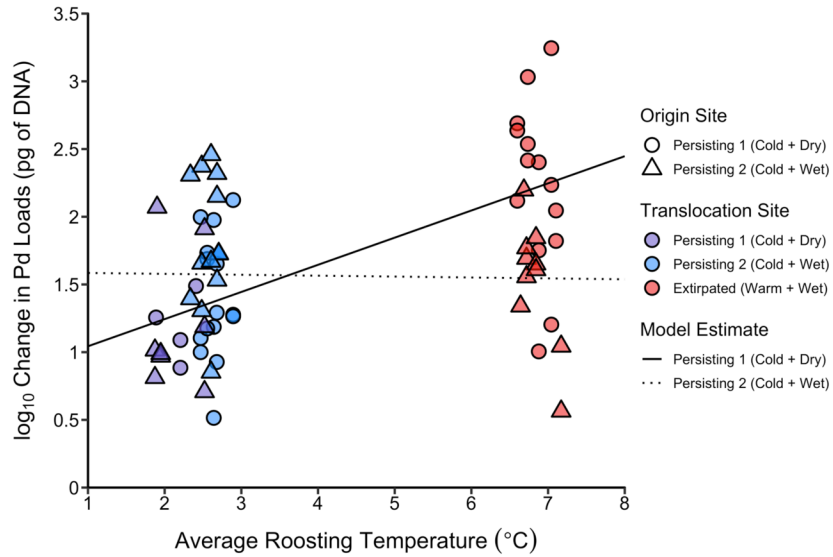


FIGURE 2: Relationship between average roosting temperature and pathogen growth rate on bats. The shape of data points denotes the persisting site from which individuals originated: Persisting 1 (Cold + Dry) = circle, Persisting 2 (Cold + Wet) = triangle. The color of data points represents the translocation sites: Persisting 1 (Cold + Dry) = purple, Persisting 2 (Cold + Wet) = blue, Extirpated (Warm + Wet) = red. The solid and dotted lines are model estimates for bats that originated in the Persisting 1 (Cold + Dry) and Persisting 2 (Cold + Wet) sites, respectively. A \log_{10} change in Pd loads value of 1 is associated with no change in pathogen load from early to late hibernation, and data points above or below this value indicate an increase or decrease in pathogen load, respectively.

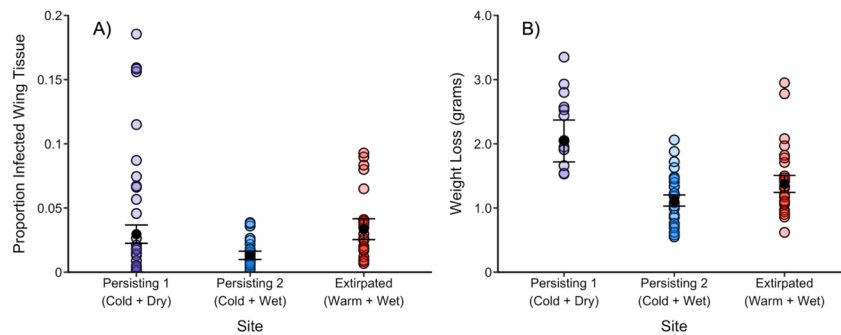


FIGURE 3: The **A)** proportion of wing tissue displaying signs of infection with *Pseudogymnoascus destructans* and **B)** amount of weight lost over hibernation in bats from each site. Tissue invasion at Extirpated (Warm + Wet) was higher than that at the similarly humid Persisting 2 (Cold + Wet), suggesting that the higher fungal growth rate at the extirpated site resulted in greater tissue invasion and ultimately higher weight loss. The low humidity conditions at Persisting 1 (Cold + Dry) may have driven the observed increase in tissue invasion despite a lower pathogen growth rate. Low humidity conditions can exacerbate evaporative water loss from infected tissue, which may have increased arousal frequency and weight loss.

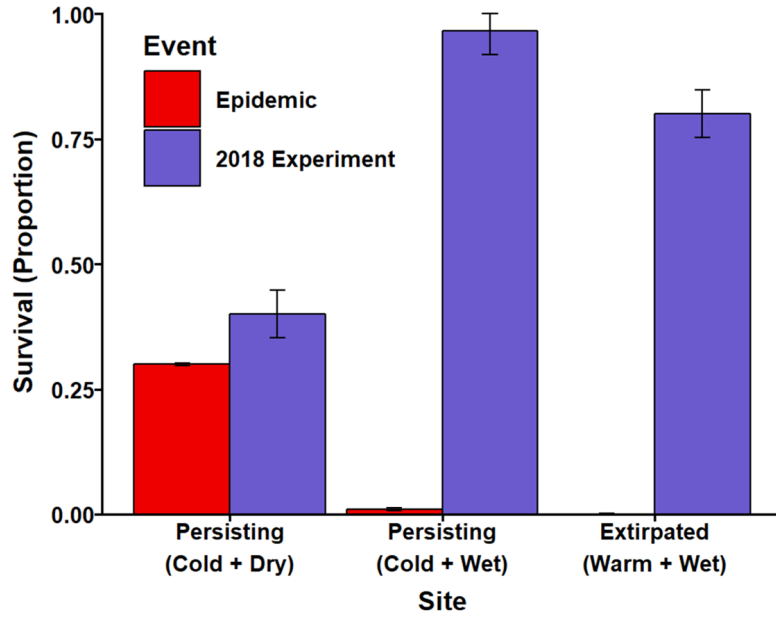


FIGURE 4: Proportion of bats surviving the initial epidemic (red bars) and 2018 experiment (blue bars) in each site. Observed survival corresponded to the degree of tissue invasion and weight loss at each site. Despite the lowest pathogen growth rate, bats in Persisting 1 (Cold + Dry) had a high degree of infection severity, ultimately resulting in the lowest observed survival. In all three sites, we observed higher survival in this experiment than during the initial epidemic within the same sites, suggesting that WNS has selected for host traits suitable to surviving the disease.

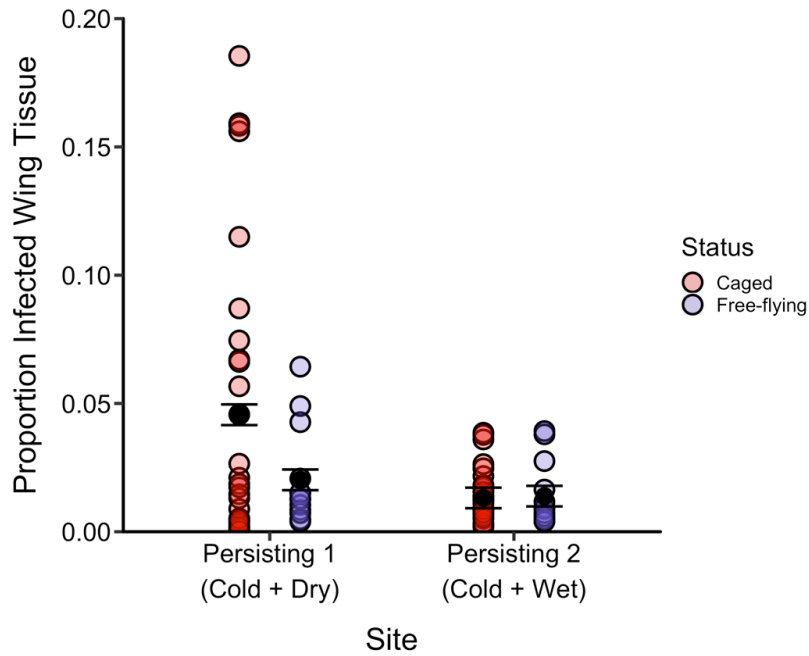
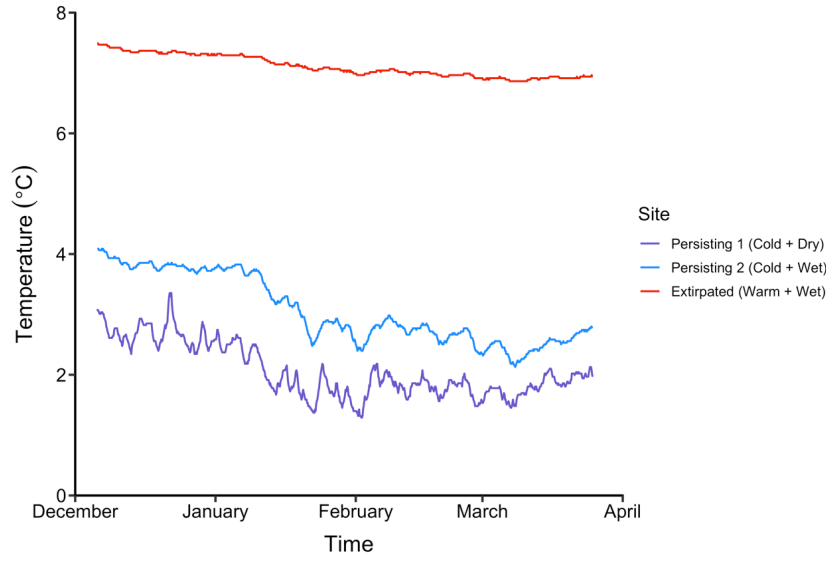
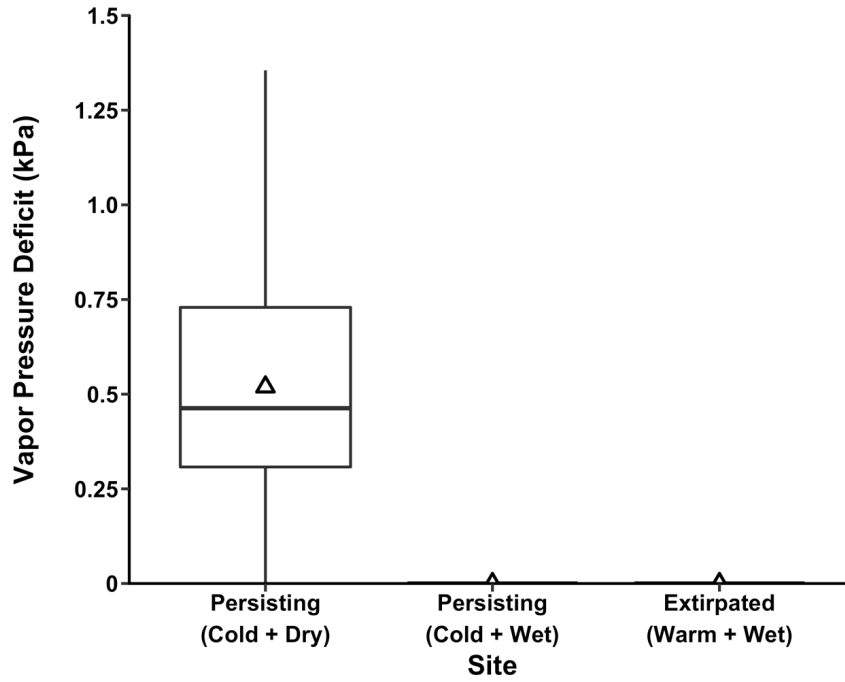


FIGURE 5: Proportion of infected wing tissue as indicated by orange fluorescence on caged and free-flying bats in each of the two persisting sites^{86,87}. Free-flying bats were opportunistically captured at the end of hibernation at experiment termination. In Persisting 1 (Cold + Dry), where disease severity in caged bats was high, caged bats had significantly higher levels of tissue invasion compared to free-flying bats within the same site. However, this difference was not detected at Persisting 2 (Cold + Wet). This suggests that little brown bats in the cold and dry persisting site do not roost in dry microclimates for the entirety of hibernation, but rather move roosting locations periodically, as has been observed prior to the WNS epidemic. Moving amongst a variety of microclimates in this site may allow this persisting colony to mitigate disease severity.

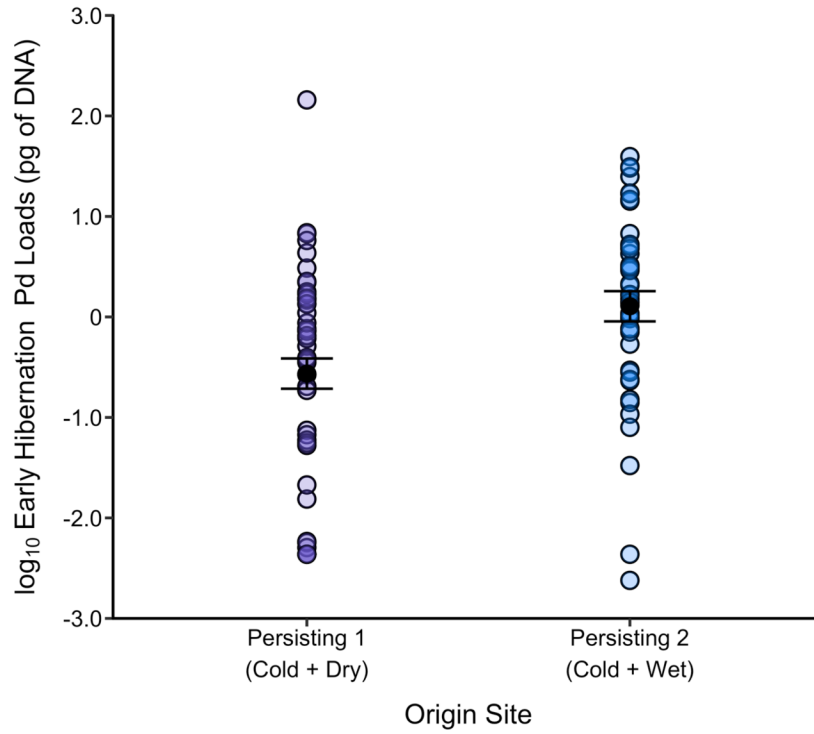


SUPPLEMENTAL FIGURES

SUPPLEMENTAL FIGURE 1: Inter-site variation in temperature, plotted over time. The average temperature in Persisting 1 (Cold + Dry), Persisting 2 (Cold + Wet), and Extirpated (Warm + Wet) sites was $2.06\text{ }^{\circ}\text{C} \pm 0.44\text{ SD}$, $3.07\text{ }^{\circ}\text{C} \pm 0.57\text{ SD}$, and $7.11\text{ }^{\circ}\text{C} \pm 0.18\text{ SD}$, respectively.

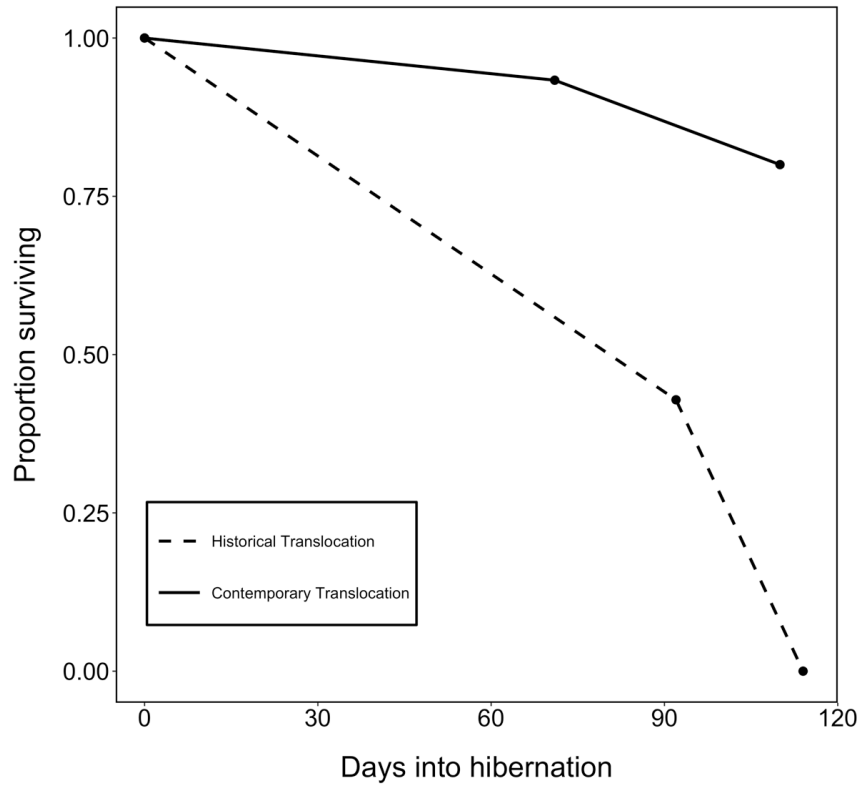


SUPPLEMENTAL FIGURE 2: Inter-site variation in vapor pressure deficit. White triangles indicate mean values. Vapor pressure deficit (VPD) is a measurement of the amount of moisture in the air and, given the temperature, its propensity to either condense or evaporate. Higher values of VPD correspond to environments in which moisture is more likely to evaporate, indicating a dry environment. The extremely low VPD values in the persisting cold and wet site and extirpated warm and wet site indicated that the air was nearly saturated and had a high propensity to condense on surfaces.

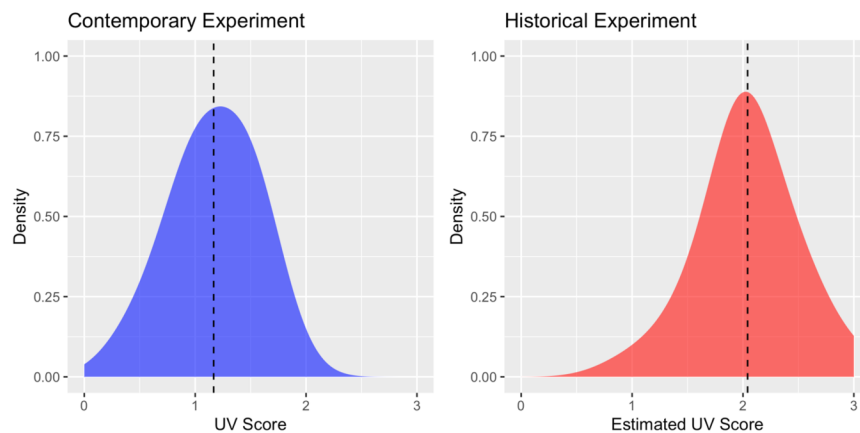


SUPPLEMENTAL FIGURE 3

Early hibernation pathogen loads (picograms of DNA). At the time of capture in December 2018, the pathogen load on bats that originated at the persisting cold and wet site were higher than those that originated in the persisting cold and dry site.

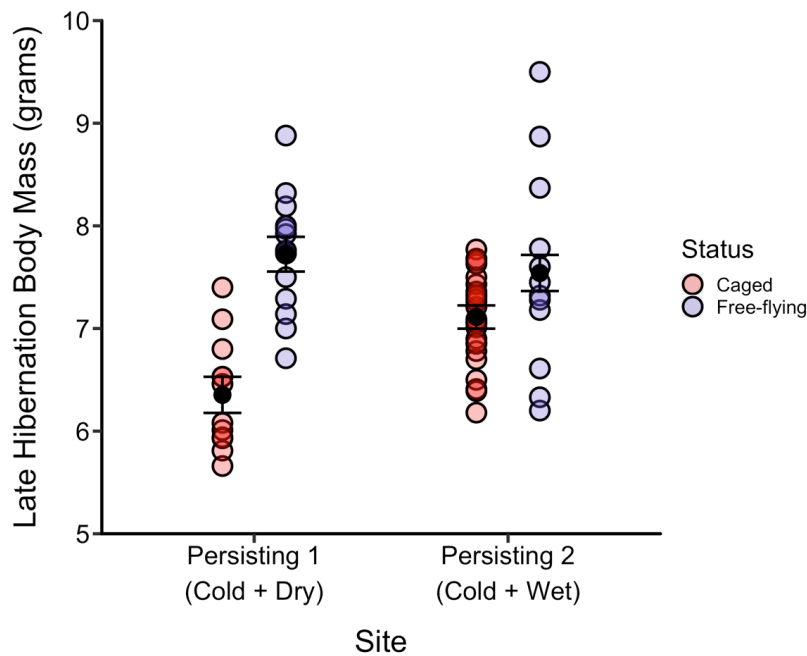


SUPPLEMENTAL FIGURE 4: Comparison of survival observed within the extirpated site during an historical translocation experiment with WNS-naïve bats in 2009 and the contemporary experiment described in this study. In the historical translocation, mortality occurred in translocated little brown bats much more rapidly compared to this study. After 114 days in the historical study, all bats succumbed to WNS, whereas in this study, the majority of bats were alive 110 days into hibernation. This strongly suggests that bats in persisting colonies have unique adaptations to surviving WNS, driving their colonies' persistence.



SUPPLEMENTAL FIGURE 5: Density plots of infection severity as indicated by degree of orange fluorescence under ultraviolet light in bats from the historical and contemporary translocation experiments in

Extirpated (Warm + Wet). A UV score of 0 = no orange fluorescence indicative of infection, 1 = 1-10% of wing area displays orange fluorescence, 2 = 10-50% of wing area displays fluorescence, and 3 = 50-100% of wing area displays fluorescence. Following mortality, bats in the historical experiment were histologically examined and infection severity scored using the following scale: 0 = no fungi suggestive of WNS, 1 = superficial and limited but suspicious of early WNS with hyphae in keratin and randomly into epidermis, but not yet forming distinctive cupping or dense packets, 2 = more extensive superficial infection with epidermal cupping packed with hyphae diagnostic of WNS, 3 = more severe fungal infection with tissue invasion including epidermal cupping packed with hyphae diagnostic of WNS, 4 = severe infection with tissue and wing damage worse than 3. To estimate UV score from the historical dataset, we assigned histology scores of 0 and 1 a UV score of 0, scores of 2 a UV score of 1, scores of 3 a UV score of 2, and scores of 4 a UV score of 3. Tissue does not display orange fluorescence until infection has been well established, and a histology score of 2 likely corresponds to when fluorescence will first be detected. Dashed lines correspond to the mean UV scores in each dataset.



SUPPLEMENTAL FIGURE 6: Late hibernation body mass in both caged and free-flying bats at both of the persisting colonies. Free-flying bats were sampled from the area of the mine where the cages were installed at the end of the experiment. At the cold and dry persisting site, where disease severity was high, caged bats had significantly lower late hibernation body weights compared to free-flying bats.



SUPPLEMENTAL FIGURE 7: Cage installation in the mines. Ten cages were installed in each site, and each contained three bats, all males and all having originated in the same persisting site. Each cage had a poultry waterer at the bottom of the cage to provide access to water as needed. Cages were predator-proofed by placing them high on ceilings and filling in gaps between cage and substrate with foam sealant.

Response variable: change in fungal loads

Multiple linear regression

Model reference level: persisting (cold + dry) translocation site, persisting (cold + dry) origin site

N = 65 (bats that were found dead at the end of the experiment were not used in this analysis)

<i>Term</i>	<i>Estimate</i>	<i>Standard Error</i>	<i>P value</i>
Intercept	1.180	0.250	<0.001
Site(Persisting Cold + Wet)	0.214	0.281	0.449
Site(Extirpated Warm + Wet)	1.045	0.283	<0.001
Origin Site(Persisting Cold + Wet)	0.028	0.306	0.928
Site(Persisting Cold + Wet):Origin Site(Persisting Cold + Wet)	0.378	0.358	0.296
Site(Extirpated Warm + Wet):Origin Site(Persisting Cold + Wet)	-0.726	0.370	0.054

SUPPLEMENTAL TABLE 1: Model output of a multiple linear regression exploring the role of both origin site and translocation site on the change in fungal loads over the course of the experiment.

Response variable: change in fungal loads

Linear mixed effects model

Model reference level: persisting (cold + dry) origin site

N = 65 (bats that were found dead at the end of the experiment were not used in this analysis)

<i>Term</i>	<i>Estimate</i>	<i>Standard Error</i>	<i>P value</i>
Intercept	0.844	0.220	0.001
Average roosting temperature	0.200	0.045	<0.001
Origin Site(Persisting Cold + Wet)	0.745	0.300	0.022
Average roosting temperature:Origin Site(Persisting Cold + Wet)	-0.207	0.065	0.005

SUPPLEMENTAL TABLE 2: Model output of a linear mixed effects model exploring the role of both origin site and average roosting temperature on the change in fungal loads over the course of the experiment.

Response variable: infection severity

Generalized linear mixed model with binomial error distribution and logit link function. Cage ID incorporated as random effect.

Model reference level: persisting (cold + dry) translocation site

N = 81 (both alive and dead bats were used for this analysis. 8 dead bats were too decomposed to successfully investigate infection severity, and the photographs from 1 alive bat were of too low quality to use in these analyses)

<i>Term</i>	<i>Estimate</i>	<i>Standard Error</i>	<i>P value</i>
Intercept	-3.536	0.242	<0.001
Site(Persisting Cold + Wet)	-0.795	0.344	0.021
Site(Extirpated Warm + Wet)	0.135	0.343	0.694

SUPPLEMENTAL TABLE 3: Model output of a generalized linear mixed model (binomial error distribution, logit link) used to explore how infection severity differed between sites.

Response variable: weight loss
Generalized linear mixed model with gamma error distribution and log link function. Cage ID incorporated as random effect.

Model reference level: persisting (cold + dry) translocation site

N = 65 (only data from bats alive at the end of the experiment was used in this analysis)

<i>Term</i>	<i>Estimate</i>	<i>Standard Error</i>	<i>P value</i>
Intercept	0.777	0.129	<0.001
Site(Persisting Cold + Wet)	-0.662	0.159	<0.001
Site(Extirpated Warm + Wet)	-0.455	0.161	0.005

SUPPLEMENTAL TABLE 4: Model output of a generalized linear mixed model (gamma error distribution, log link function) used to explore how host body condition differed between sites.

Response variable: survival
Generalized linear mixed model with binomial error distribution and logit link function. Cage ID incorporated as random effect.

Model reference level: persisting (cold + dry) translocation site

N = 90 (all experimental bats were used in this analysis)

<i>Term</i>	<i>Estimate</i>	<i>Standard Error</i>	<i>P value</i>
Intercept	-0.495	0.526	0.346
Site(Persisting Cold + Wet)	4.262	1.337	0.001
Site(Extirpated Warm + Wet)	2.162	0.894	0.016

SUPPLEMENTAL TABLE 5: Model output of a generalized linear mixed model (binomial error distribution, logit link function) used to explore how host survival differed between sites.

Response variable: survival
Generalized linear mixed model with binomial error distribution and logit link function. Cage ID incorporated as random effect.

N = 90 (all experimental bats were used in this analysis)

<i>Term</i>	<i>Estimate</i>	<i>Standard Error</i>	<i>P value</i>
Intercept	1.864	4.314	0.666
Early hibernation body mass	-0.026	0.511	0.959

SUPPLEMENTAL TABLE 6: Model output of a generalized linear mixed model (binomial error distribution, logit link function) used to explore how the relationship between early hibernation body mass and host survival.

Response variable: infection severity			
<i>Generalized linear model with binomial error distribution and logit link function.</i>			
<i>Model reference level: persisting (cold + dry) translocation site, free-flying bats</i>			
<i>N = 78 (both alive and dead bats in cages were used for this analysis, excluding data from the extirpated site. Data from 58 caged bats from the two persisting sites as well as 20 free-flying bats were used in this analysis. Data from 10 free-flying bats was collected at each of the two persisting sites)</i>			
<i>Term</i>	<i>Estimate</i>	<i>Standard Error</i>	<i>P value</i>
Intercept	-3.776	0.002	<0.001
Site(Persisting Cold + Wet)	-0.486	0.002	<0.001
Caged(Yes)	0.676	0.002	<0.001
Site(Persisting Cold + Wet):Caged(Yes)	-0.743	0.002	<0.001

SUPPLEMENTAL TABLE 7: Model output of a generalized linear model (binomial error distribution, logit link) used to explore how infection severity differed between caged and free-flying bats in each of the two persisting sites.

Response variable: late hibernation body mass			
<i>Multiple linear regression</i>			
<i>Model reference level: persisting (cold + dry) translocation site, free-flying bats</i>			
<i>N = 66 (Data from 41 alive, caged bats from the two persisting sites as well as 25 free-flying bats were used in this analysis. No data from the extirpated site was used. Late hibernation body mass data from 12 and 13 free-flying bats was collected at the cold/wet and cold/dry persisting sites, respectively)</i>			
<i>Term</i>	<i>Estimate</i>	<i>Standard Error</i>	<i>P value</i>
Intercept	7.724	0.169	<0.001
Site(Persisting Cold + Wet)	-0.183	0.244	0.456
Caged(Yes)	-1.371	0.244	<0.001
Site(Persisting Cold + Wet):Caged(Yes)	0.941	0.322	0.005

SUPPLEMENTAL TABLE 8: Model output of a multiple linear regression used to explore how late hibernation body mass differed between caged and free-flying bats in each of the two persisting sites.

ACKNOWLEDGEMENTS

We would like to thank several individuals for their invaluable contributions to the field element of this study. From the New York State Department of Environmental Conservation (NYDEC), we would like to thank Amanda Bailey, Samantha Hoff, and Casey Pendergast. From the Vermont Fish & Wildlife Department, we

thank Kerry Monahan and Joel Flewelling. Funding was provided by the joint NSF-NIH-NIFA Ecology and Evolution of Infectious Disease award DEB-1911853 and Virginia Tech.

REFERENCES

1. Antolin, M. F., Gober, P., Luce, B., Biggins, D. E. & Van Pelt, W. E. The Influence of Sylvatic Plague on North American Wildlife at the Landscape Level, with Special Emphasis on Black-footed Ferret and Prairie Dog Conservation. *US Fish Wildl. Publ.* **57** , 104–127 (2002).
2. LaDeau, S. L., Kilpatrick, A. M. & Marra, P. P. West Nile virus emergence and large-scale declines of North American bird populations. *Nature* **447** , 710–713 (2007).
3. Langwig, K. E. *et al.* Sociality, density-dependence and microclimates determine the persistence of populations suffering from a novel fungal disease, white-nose syndrome. *Ecol. Lett.* **15** , 1050–1057 (2012).
4. McCallum, H. *et al.* Transmission dynamics of Tasmanian devil facial tumor disease may lead to disease-induced extinction. *Ecology* **90** , 3379–3392 (2009).
5. Scheele, B. C. *et al.* Amphibian fungal panzootic causes catastrophic and ongoing loss of biodiversity. *Science (80-.)*. **363** , 1459–1463 (2019).
6. Van Riper III, C., Van Riper, S. G., Goff, M. L. & Laird, M. The Epizootiology and Ecological Significance of Malaria in Hawaiian Land Birds. *Ecol. Monogr.* **56** , 327–344 (1986).
7. de Castro, F. & Bolker, B. Mechanisms of disease-induced extinction. *Ecol. Lett.* **8** , 117–126 (2005).
8. Friedman, A. & Yakubu, A.-A. HOST DEMOGRAPHIC ALLEE EFFECT, FATAL DISEASE, AND MIGRATION: PERSISTENCE OR EXTINCTION. *SIAM J. Appl. Math.* **72** , 1644–1666 (2012).
9. Lande, R. Demographic Stochasticity and Allee Effect on a Scale with Isotropic Noise. *Oikos* **83** , 353–358 (1998).
10. Brannelly, L. A. *et al.* Mechanisms underlying host persistence following amphibian disease emergence determine appropriate management strategies. *Ecol. Lett.* **24** , 130–148 (2021).
11. Briggs, C. J., Knapp, R. A. & Vredenburg, V. T. Enzoootic and epizootic dynamics of the chytrid fungal pathogen of amphibians. *Proc. Natl. Acad. Sci.* **107** , 9695–9700 (2010).
12. Voyles, J. *et al.* Shifts in disease dynamics in a tropical amphibian assemblage are not due to pathogen attenuation. *Science (80-.)*. **359** , 1517–1519 (2018).
13. Scheele, B. C., Hunter, D. A., Skerratt, L. F., Brannelly, L. A. & Driscoll, D. A. Low impact of chytridiomycosis on frog recruitment enables persistence in refuges despite high adult mortality. *Biol. Conserv.* **182** , 36–43 (2015).
14. Scheele, B. C. *et al.* After the epidemic: Ongoing declines, stabilizations and recoveries in amphibians afflicted by chytridiomycosis. *Biol. Conserv.* **206** , 37–46 (2017).
15. Epstein, B. *et al.* Rapid evolutionary response to a transmissible cancer in Tasmanian devils. *Nat. Commun.* **7** , 12684 (2016).
16. Lazenby, B. T. *et al.* Density trends and demographic signals uncover the long-term impact of transmissible cancer in Tasmanian devils. *J. Appl. Ecol.* **55** , 1368–1379 (2018).
17. Patton, A. H. *et al.* A transmissible cancer shifts from emergence to endemism in Tasmanian devils. *Science (80-.)*. **370** , eabb9772 (2020).
18. Hohenlohe, P. A. *et al.* Conserving adaptive potential: lessons from Tasmanian devils and their transmissible cancer. *Conserv. Genet.* **20** , 81–87 (2019).

19. Woodworth, B. L. *et al.* Host population persistence in the face of introduced vector-borne diseases: Hawaii amakihi and avian malaria. *Proc. Natl. Acad. Sci.* **102** , 1531–1536 (2005).
20. Reichard, J. D. *et al.* Interannual Survival of *Myotis lucifugus* (Chiroptera: Vespertilionidae) near the Epicenter of White-Nose Syndrome. *Northeast. Nat.* **21** , N56–N59 (2014).
21. Frick, W. F. *et al.* Disease alters macroecological patterns of North American bats. *Glob. Ecol. Biogeogr.* **24** , 741–749 (2015).
22. Hoyt, J. R. *et al.* Environmental reservoir dynamics predict global infection patterns and population impacts for the fungal disease white-nose syndrome. *Proc. Natl. Acad. Sci.* **117** , 7255–7262 (2020).
23. Hoyt, J. R., Kilpatrick, A. M. & Langwig, K. E. Ecology and impacts of white-nose syndrome on bats. *Nat. Rev. Microbiol.* **19** , 1–15 (2021).
24. Langwig, K. E. *et al.* Drivers of variation in species impacts for a multi-host fungal disease of bats. *Philos. Trans. R. Soc. B Biol. Sci.* **371** , 20150456 (2016).
25. Samuel, M. D., Woodworth, B. L., Atkinson, C. T., Hart, P. J. & LaPointe, D. A. Avian malaria in Hawaiian forest birds: Infection and population impacts across species and elevations. *Ecosphere* **6** , 1–21 (2015).
26. Scheele, B. C. *et al.* After the epidemic: Ongoing declines, stabilizations and recoveries in amphibians afflicted by chytridiomycosis. *Biol. Conserv.* **206** , 37–46 (2017).
27. Best, A., White, A. & Boots, M. Maintenance of host variation in tolerance to pathogens and parasites. *Proc. Natl. Acad. Sci.* **105** , 20786–20791 (2008).
28. Boots, M., Best, A., Miller, M. R. & White, A. The role of ecological feedbacks in the evolution of host defence: what does theory tell us? *Philos. Trans. R. Soc. B* **364** , 27–36 (2009).
29. Kutzer, M. A. M. & Armitage, S. A. O. Maximising fitness in the face of parasites: a review of host tolerance. *Zoology* **119** , 281–289 (2016).
30. Råberg, L., Sim, D. & Read, A. F. Disentangling Genetic Variation for Resistance and Tolerance to Infectious Diseases in Animals. *Science (80-.)*. **318** , 812–814 (2007).
31. Råberg, L., Graham, A. L. & Read, A. F. Decomposing health: tolerance and resistance to parasites in animals. *Philos. Trans. R. Soc. B Biol. Sci.* **364** , 37–49 (2009).
32. Restif, O. & Koella, J. C. Concurrent Evolution of Resistance and Tolerance to Pathogens. *Am. Nat.* **164** , E90–E102 (2004).
33. Roy, B. A. & Kirchner, J. W. Evolutionary Dynamics of Pathogen Resistance and Tolerance. *Evolution (N. Y.)*. **54** , 51–63 (2000).
34. Voyles, J. *et al.* Shifts in disease dynamics in a tropical amphibian assemblage are not due to pathogen attenuation. *Science (80-.)*. **359** , 1517–1519 (2018).
35. Wilber, M. Q., Carter, E. D., Gray, M. J. & Briggs, C. J. Putative resistance and tolerance mechanisms have little impact on disease progression for an emerging salamander pathogen. *Funct. Ecol.* **35** , 847–859 (2021).
36. Heard, G. W. *et al.* Refugia and connectivity sustain amphibian metapopulations afflicted by disease. *Ecol. Lett.* **18** , 853–863 (2015).
37. Mosher, B. A., Bailey, L. L., Muths, E. & Huyvaert, K. P. Host–pathogen metapopulation dynamics suggest high elevation refugia for boreal toads. *Ecol. Appl.* **28** , 926–937 (2018).
38. Schelkle, B. *et al.* Parasites pitched against nature: Pitch Lake water protects guppies (*Poecilia reticulata*) from microbial and gyrodactylid infections. *Parasitology* **139** , 1772–1779 (2012).

39. Springer, Y. P. Do extreme environments provide a refuge from pathogens? A phylogenetic test using serpentine flax. *Am. J. Bot.***96** , 2010–2021 (2009).
40. Tobler, M., Schlupp, I., García De León, F. J., Glaubrecht, M. & Plath, M. Extreme habitats as refuge from parasite infections? Evidence from an extremophile fish. *Acta Oecologica* **31** , 270–275 (2007).
41. Zumbado-Ulate, H., Bolaños, F., Gutiérrez-Espeleta, G. & Puschendorf, R. Extremely Low Prevalence of *Batrachochytrium dendrobatidis* in Frog Populations from Neotropical Dry Forest of Costa Rica Supports the Existence of a Climatic Refuge from Disease. *Ecohealth* **11** , 593–602 (2014).
42. Arthur, A., Ramsey, D. & Efford, M. Impact of bovine tuberculosis on a population of brushtail possums (*Trichosurus vulpecula* Kerr) in the Orongorongo Valley, New Zealand. *Wildl. Res.* **31** , 389–395 (2004).
43. Lachish, S., McCallum, H. & Jones, M. Demography, disease and the devil: Life-history changes in a disease-affected population of Tasmanian devils (*Sarcophilus harrisii*). *J. Anim. Ecol.***78** , 427–436 (2009).
44. McDonald, J. L. *et al.* Demographic buffering and compensatory recruitment promotes the persistence of disease in a wildlife population. *Ecol. Lett.* **19** , 443–449 (2016).
45. Spitzen-Van Der Sluijs, A., Canessa, S., Martel, A. & Pasmans, F. Fragile coexistence of a global chytrid pathogen with amphibian populations is mediated by environment and demography. *Proc. R. Soc. B Biol. Sci.* **284** , 20171444 (2017).
46. Fenton, A., Fairbairn, J. P., Norman, R. & Hudson, P. J. Parasite transmission: reconciling theory and reality. *J. Anim. Ecol.***71** , 893–905 (2002).
47. Hochachka, W. M. & Dhondt, A. A. Density-dependent decline of host abundance resulting from a new infectious disease. *Proc. Natl. Acad. Sci.* **97** , 5303–5306 (2000).
48. Lloyd-Smith, J. O. *et al.* Should we expect population thresholds for wildlife disease? *Trends Ecol. Evol.* **20** , 511–519 (2005).
49. McCallum, H., Barlow, N. & Hone, J. How should pathogen transmission be modelled? *Trends Ecol. Evol.* **16** , 295–300 (2001).
50. Anderson, R. M. & May, R. M. Coevolution of hosts and parasites. *Parasitology* **85** , 411–426 (1982).
51. Boots, M., Hudson, P. J. & Sasaki, A. Large shifts in pathogen virulence relate to host population structure. *Science (80-)*.**303** , 842–844 (2004).
52. CRESSLER, C. E., McLEOD, D. V., ROZINS, C., VAN DEN HOOGEN, J. & DAY, T. The adaptive evolution of virulence: a review of theoretical predictions and empirical tests. *Parasitology* **143** , 915–930 (2016).
53. Kerr, B., Neuhauser, C., Bohannan, B. J. M. & Dean, A. M. Local migration promotes competitive restraint in a host-pathogen ‘tragedy of the commons’. *Nature* **442** , 75–78 (2006).
54. Levin, S. & Pimentel, D. Selection of Intermediate Rates of Increase in Parasite-Host Systems. *Am. Nat.* **117** , 308–315 (1981).
55. Wild, G., Gardner, A. & West, S. A. Adaptation and the evolution of parasite virulence in a connected world. *Nature* **459** , 983–986 (2009).
56. Lorch, J. M. *et al.* Experimental infection of bats with *Geomyces destructans* causes white-nose syndrome. *Nature***480** , 376–379 (2011).
57. Minnis, A. M. & Lindner, D. L. Phylogenetic evaluation of *Geomyces* and allies reveals no close relatives of *Pseudogymnoascus destructans*, comb. nov., in bat hibernacula of eastern North America. *Fungal Biol.* **117** , 638–649 (2013).

58. Warnecke, L. *et al.* Inoculation of bats with European *Geomyces destructans* supports the novel pathogen hypothesis for the origin of white-nose syndrome. *Proc. Natl. Acad. Sci.* **109** , 6999–7003 (2012).
59. Blehert, D. S. *et al.* Bat white-nose syndrome: An emerging fungal pathogen? *Science (80-.)*. **323** , 227 (2009).
60. Langwig, K. E. *et al.* Host and pathogen ecology drive the seasonal dynamics of a fungal disease, white-nose syndrome. *Proc. R. Soc. B* **282** , 20142335 (2015).
61. Hoyt, J. R. *et al.* Cryptic connections illuminate pathogen transmission within community networks. *Nature* **563** , 710–713 (2018).
62. Langwig, K. E. *et al.* Mobility and infectiousness in the spatial spread of an emerging fungal pathogen. *J. Anim. Ecol.* 1–8 (2021) doi:10.1111/1365-2656.13439.
63. Frick, W. F. *et al.* An emerging disease causes regional population collapse of a common North America bat species. *Science (80-.)*. **329** , 679–682 (2010).
64. Fuller, N. W. *et al.* Disease recovery in bats affected by white-nose syndrome. *J. Exp. Biol.* **223** , jeb211912 (2020).
65. Meteyer, C. U. *et al.* Recovery of Little Brown Bats (*Myotis Lucifugus*) From Natural Infection With *Geomyces Destructans*, White-Nose Syndrome. *J. Wildl. Dis.* **47** , 618–626 (2011).
66. Verant, M. L., Boyles, J. G., Waldrep Jr., W., Wibbelt, G. & Blehert, D. S. Temperature-Dependent Growth of *Geomyces destructans*, the Fungus That Causes Bat White-Nose Syndrome. *PLoS One* **7** , e46280 (2012).
67. Marroquin, C. M., Lavine, J. O. & Windstam, S. T. Effect of Humidity on Development of *Pseudogymnoascus destructans* , the Causal Agent of Bat White-Nose Syndrome. *Northeast. Nat.* **24** , 54–64 (2017).
68. Grieneisen, L. E., Brownlee-Bouboulis, S. A., Johnson, J. S. & Reeder, D. M. Sex and hibernaculum temperature predict survivorship in white-nose syndrome affected little brown myotis (*Myotis lucifugus*). *R. Soc. Open Sci.* **2** , 140470 (2015).
69. Hopkins, S. R. *et al.* Continued preference for suboptimal habitat reduces bat survival with white-nose syndrome. *Nat. Commun.* **12** , 1–9 (2021).
70. Lilley, T. M., Anttila, J. & Ruokolainen, L. Landscape structure and ecology influence the spread of a bat fungal disease. *Funct. Ecol.* **32** , 2483–2496 (2018).
71. Dobony, C. A. *et al.* Little Brown Myotis Persist Despite Exposure to White-Nose Syndrome. *J. Fish Wildl. Manag.* **2** , 190–195 (2011).
72. Langwig, K. E. *et al.* Resistance in persisting bat populations after white-nose syndrome invasion. *Philos. Trans. R. Soc. B* **372** , 20160044 (2017).
73. Drees, K. P. *et al.* Phylogenetics of a fungal invasion: origins and widespread dispersal of white-nose syndrome. *MBio* **8** , e01941-17 (2017).
74. Palmer, J. M. *et al.* Molecular characterization of a heterothallic mating system in *Pseudogymnoascus destructans*, the fungus causing white-nose syndrome of bats. *G3 Genes, Genomes, Genet.* **4** , 1755–1763 (2014).
75. Ren, P. *et al.* Clonal spread of *Geomyces destructans* among bats, Midwestern and Southern United States. *Emerg. Infect. Dis.* **18** , 883–885 (2012).
76. Hoyt, J. R. *et al.* Host persistence or extinction from emerging infectious disease: insights from white-nose syndrome in endemic and invading regions. *Proc. R. Soc. B* **283** , 20152861 (2016).

77. Langwig, K. E. *et al.* Invasion dynamics of white-nose syndrome fungus, midwestern United States, 2012–2014. *Emerg. Infect. Dis.* **21** , 1023–1026 (2015).
78. McGuire, L. P., Mayberry, H. W. & Willis, C. K. R. White-nose syndrome increases torpid metabolic rate and evaporative water loss in hibernating bats. *Am. J. Physiol. Integr. Comp. Physiol.* **313** , R680–R686 (2017).
79. Cryan, P. M., Meteyer, C. U., Boyles, J. G. & Blehert, D. S. Wing pathology of white-nose syndrome in bats suggests life-threatening disruption of physiology. *BMC Biol.* **8** , 1–8 (2010).
80. Cryan, P. M. *et al.* Electrolyte Depletion in White-nose Syndrome Bats. *J. Wildl. Dis.* **49** , 398–402 (2013).
81. Ehlman, S. M., Cox, J. J. & Crowley, P. H. Evaporative water loss, spatial distributions, and survival in white-nose-syndrome-affected little brown myotis: a model. *J. Mammal.* **94** , 572–583 (2013).
82. Verant, M. L. *et al.* White-nose syndrome initiates a cascade of physiologic disturbances in the hibernating bat host. *BMC Physiol.* **14** , 1–11 (2014).
83. Warnecke, L. *et al.* Pathophysiology of white-nose syndrome in bats: a mechanistic model linking wing damage to mortality. *Biol. Lett.* **9** , 20130177 (2013).
84. Willis, C. K. R., Menzies, A. K., Boyles, J. G. & Wojciechowski, M. S. Evaporative Water Loss Is a Plausible Explanation for Mortality of Bats from White-Nose. *Integr. Comp. Biol.* **51** , 364–373 (2011).
85. Hicks, A. C. *et al.* Environmental transmission of *Pseudogymnoascus destructans* to hibernating little brown bats. *bioRxiv* (2021) doi:<https://doi.org/10.1101/2021.07.01.450774>.
86. Meteyer, C. U. *et al.* Histopathologic criteria to confirm white-nose syndrome in bats. *J. Vet. Diagnostic Investig.* **21** , 411–414 (2009).
87. Turner, G. G. *et al.* Nonlethal Screening of Bat-Wing Skin With the Use of Ultraviolet Fluorescence To Detect Lesions Indicative of White-Nose Syndrome. *J. Wildl. Dis.* **50** , 566–573 (2014).
88. Auteri, G. G. & Knowles, L. L. Decimated little brown bats show potential for adaptive change. *Sci. Rep.* **10** , 1–10 (2020).
89. Gignoux-Wolfsohn, S. A. *et al.* Genomic signatures of evolutionary rescue in bats surviving white-nose syndrome. *Mol. Ecol.* **In press** , (2021).
90. Valerio Garcia, M., Carlos Monteiro, A., Juan Pablo Szabo, M., Prette, N. & Henrique Bechara, G. MECHANISM OF INFECTION AND COLONIZATION OF RHIPICEPHALUS SANGUINEUS EGGS BY MERTARHIZIUM ANISOPLIAE AS REVEALED BY SCANNING ELECTRON MICROSCOPY AND HISTOPATHOLOGY. *Brazilian J. Microbiol.* **36** , 368–372 (2005).
91. Ment, D. *et al.* The effect of temperature and relative humidity on the formation of *Metarhizium anisopliae* chlamydospores in tick eggs. *Fungal Biol.* **114** , 49–56 (2010).
92. Ben-Hamo, M., Muñoz-Garcia, A., Williams, J. B., Korine, C. & Pinshow, B. Waking to drink: rates of evaporative water loss determine arousal frequency in hibernating bats. *J. Exp. Biol.* **216** , 573–577 (2013).
93. Thomas, D. W. & Cloutier, D. Evaporative Water Loss by Hibernating Little Brown Bats, *Myotis lucifugus*. *Physiol. Zool.* **65** , 443–456 (1992).
94. Reeder, D. M. *et al.* Frequent arousal from hibernation linked to severity of infection and mortality in bats with white-nose syndrome. *PLoS One* **7** , e38920 (2012).
95. Perry, R. W. A review of factors affecting cave climates for hibernating bats in temperate North America. *Environ. Rev.* **21** , 28–39 (2013).

96. Ryan, C. C., Burns, L. E. & Broders, H. G. Changes in underground roosting patterns to optimize energy conservation in hibernating bats. *Can. J. Zool.* **97** , 1064–1070 (2019).
97. Boyles, J. G., Johnson, J. S., Blomberg, A. & Lilley, T. M. Optimal hibernation theory. *Mamm. Rev.* **50** , 91–100 (2020).
98. Boyles, J. G., Boyles, E., Dunlap, R. K., Johnson, S. A. & Brack Jr, V. Long-term microclimate measurements add further evidence that there is no ‘optimal’ temperature for bat hibernation. *Mamm. Biol.* **86** , 9–16 (2017).
99. McKenzie, J. M., Price, S. J., Connette, G. M., Bonner, S. J. & Lorch, J. M. Effects of snake fungal disease on short-term survival, behavior, and movement in free-ranging snakes. *Ecol. Appl.* **31** , e02251 (2021).
100. Lorch, J. M. *et al.* Experimental Infection of Snakes with *Ophidiomyces ophiodiicola* Causes Pathological Changes That Typify Snake Fungal Disease. *MBio* **6** , e01534-15 (2015).
101. Burns, G., Ramos, A. & Muchlinski, A. Fever Response in North American Snakes. *Source J. Herpetol.* **30** , 133–139 (1996).
102. Bell, G. Evolutionary rescue and the limits of adaptation. *Philos. Trans. R. Soc. B Biol. Sci.* **368** , 20120080 (2013).
103. Auteri, G. G. & Knowles, L. L. Decimated little brown bats show potential for adaptive change. *Sci. Rep.* **10** , (2020).
104. Lilley, T. M. *et al.* Genome-Wide Changes in Genetic Diversity in a Population of *Myotis lucifugus* Affected by White-Nose Syndrome. *Genes, Genomes, Genet.* **10** , 2007–2020 (2020).
105. Felsenstein, J. THE THEORETICAL POPULATION GENETICS OF VARIABLE SELECTION AND MIGRATION. *Annu. Rev. Genet.* **10** , 253–280 (1976).
106. Garcia-Ramos, G. & Kirkpatrick, M. GENETIC MODELS OF ADAPTATION AND GENE FLOW IN PERIPHERAL POPULATIONS. *Evolution (N. Y.)*. **51** , 21–28 (1997).
107. Hendry, A. P., Day, T. & Taylor, E. B. Population mixing and the adaptive divergence of quantitative traits in discrete populations: a theoretical framework for empirical tests. *Evolution (N. Y.)*. **55** , 459–466 (2001).
108. Wright, S. *Evolution and the Genetics of Populations, Volume 2: The Theory of Gene Frequencies* . (University of Chicago Press, 1969).
109. Johnson, L. N. L. *et al.* Population Genetic Structure Within and among Seasonal Site Types in the Little Brown Bat (*Myotis lucifugus*) and the Northern Long-Eared Bat (*M. septentrionalis*). *PLoS One* **10** , e0126309 (2015).
110. Talbot, B., Vonhof, M. J., Broders, H. G., Fenton, M. B. & Keyghobadi, N. Population structure in two geographically sympatric and congeneric ectoparasites (*Cimex adjunctus* and *cimex lectularius*) in the North American great lakes region. *Can. J. Zool.* **95** , 901–907 (2017).
111. Talbot, B., Vonhof, M. J., Broders, H. G., Fenton, B. & Keyghobadi, N. Range-wide genetic structure and demographic history in the bat ectoparasite *Cimex adjunctus*. *BMC Evol. Biol.* **16** , 1–13 (2016).
112. Burns, L. E., Frasier, T. R. & Broders, H. G. Genetic connectivity among swarming sites in the wide ranging and recently declining little brown bat (*Myotis lucifugus*). *Ecol. Evol.* **4** , 4130–4149 (2014).
113. Wilder, A. P., Kunz, T. H. & Sorenson, M. D. Population genetic structure of a common host predicts the spread of white-nose syndrome, an emerging infectious disease in bats. *Mol. Ecol.* **24** , 5495–5506 (2015).

114. Davy, C. M., Martinez-Nunez, F., Willis, C. K. R. & Good, S. V. Spatial genetic structure among bat hibernacula along the leading edge of a rapidly spreading pathogen. *Conserv. Genet.* **16** , 1013–1024 (2015).
115. Miller-Butterworth, C. M., Vonhof, M. J., Rosenstern, J., Turner, G. G. & Russell, A. L. Genetic Structure of Little Brown Bats (*Myotis lucifugus*) Corresponds with Spread of White-Nose Syndrome among Hibernacula. *J. Hered.* **105** , 354–364 (2014).
116. Price, S. J. *et al.* Effects of historic and projected climate change on the range and impacts of an emerging wildlife disease. *Glob. Chang. Biol.* **25** , 2648–2660 (2019).
117. Altizer, S., Ostfeld, R. S., Johnson, P. T. J., Kutz, S. & Harvell, C. D. Climate Change and Infectious Diseases: From Evidence to a Predictive Framework. *Science (80-.)*. **341** , 514–519 (2013).
118. Parratt, S. R., Numminen, E. & Laine, A.-L. Infectious Disease Dynamics in Heterogeneous Landscapes. *Annu. Rev. Ecol. Evol. Syst.* **47** , 283–306 (2016).
119. Wilber, M. Q., Langwig, K. E., Kilpatrick, A. M., Mccallum, H. I. & Briggs, C. J. Integral Projection Models for host-parasite systems with an application to amphibian chytrid fungus. *Methods Ecol. Evol.* **7** , 1182–1194 (2016).
120. Barrett, R. D. H. & Schluter, D. Adaptation from standing genetic variation. *Trends Ecol. Evol.* **23** , 38–44 (2008).
121. Wolinska, J. & King, K. C. Environment can alter selection in host–parasite interactions. *Trends Parasitol.* **25** , 236–244 (2009).
122. Muller, L. K. *et al.* Bat white-nose syndrome: a real-time TaqMan polymerase chain reaction test targeting the intergenic spacer region of *Geomyces destructans* . *Mycologia* **105** , 253–259 (2013).
123. Bates, D., Machler, M., Bolker, B. M. & Walker, S. C. Fitting linear mixed-effects models using lme4. *J. Stat. Softw.* **67** , 1–48 (2015).